

## Effects of heat treatment on phase contents and mechanical properties of infiltrated B<sub>4</sub>C/2024Al composites

Xiao-fen TAN<sup>1</sup>, Fan-hao ZENG<sup>1</sup>, Shu-qiu WANG<sup>1</sup>, Fei ZHOU<sup>2</sup>, Xiang XIONG<sup>1</sup>

1. State Key laboratory of Powder Metallurgy, Powder Metallurgy Research Institute,  
Central South University, Changsha 410083, China;

2. School of Materials Science and Engineering, Central South University, Changsha 410083, China

Received 17 October 2013; accepted 14 April 2014

**Abstract:** The B<sub>4</sub>C/2024Al composites were successfully produced by pressureless infiltration method, and the effects of heat treatment on phase content and mechanical properties were investigated by X-ray diffraction (XRD), scanning electron microscopy (SEM) and mechanical properties testing. The results show that phases of B<sub>4</sub>C/2024Al composites include B<sub>4</sub>C, Al, Al<sub>3</sub>BC, AlB<sub>2</sub> and Al<sub>2</sub>Cu. The phase species remain unchanged; however, the phase content of the composites changes significantly after heat treatment at the temperature of 660, 700, 800 or 900 °C for 12, 24 or 36 h. It is found that the heat treatment results in not only considerable enhancement in hardness, but also reduction in bending strength of the composites. Heat treatment at 800 °C for 36 h does best to hardness of the composites, while at 700 °C for 36 h it is the most beneficial to their comprehensive mechanical properties.

**Key words:** B<sub>4</sub>C/2024Al composites; heat treatment; pressureless infiltration; hardness; bending strength

### 1 Introduction

Boron carbide (B<sub>4</sub>C) is regarded as an important ceramic for its excellent properties including low density (2.52 g/cm<sup>3</sup>), high melting point (2450 °C), high hardness (35–45 GPa) and chemical inertness [1–3]. However, the brittleness of the B<sub>4</sub>C ( $K_{IC} < 2.2 \text{ MPa}\cdot\text{m}^{1/2}$ ) has limited its widespread applications. To improve the toughness, many metals, such as aluminum (Al), magnesium (Mg), titanium (Ti), copper (Cu) and iron (Fe), have been used as binders to form B<sub>4</sub>C-M composites.

Owing to the low density and low melting point, Al is widely used as a metal binder to increase the fracture toughness of B<sub>4</sub>C and the fabrication of these composites usually has a cost-effective manner through pressureless melt infiltration. Pressureless infiltration process [4–6] has many advantages over the widely used hot pressing method in the production of monolithic B<sub>4</sub>C. In hot pressing, it is inherently more difficult to form shapes than other flat plates. In addition, processing costs are much higher compared with pressureless melt infiltration. In the present work, pressureless infiltration

method is used to prepare the desired composites with relatively low cost.

B<sub>4</sub>C/Al composites [7,8] are potential to act as armour materials in body protection, helicopters, military air-crafts and vehicles to which light weight is of topmost significance. For the above applications, mechanical properties including hardness, bending strength, compressive strength, elastic modulus and fracture toughness require balancing cautiously along with low density and a homogeneous microstructure which is nearly free of pores.

Many researchers have investigated the fabrication process and mechanical properties of B<sub>4</sub>C/Al composites. KISASOZ et al [9] investigated the production of A6063/SiC–B<sub>4</sub>C hybrid composites using vacuum assisted block mould investment casting. WESTERMANN et al [10] investigated the effect of quenching rate on aluminium alloy. PYZIK et al [11] produced boron carbide–aluminum composites with homogeneous microstructure, which possesses desired mechanical properties. VIALA et al [12] studied the chemical reactions between B<sub>4</sub>C and Al under the temperature of 627–1000 °C. LÜ et al [13] and LEE and KANG [14] have improved mechanical properties of B<sub>4</sub>C/Al composites by in-situ

synthesis of  $\text{TiB}_2$  phases. TUNCER et al [15] reported that the infiltration process of aluminum alloy could be promoted by employing thermal passivation treatment on porous ceramics skeleton, which lowered reactivity of  $\text{B}_4\text{C}$  and decreased the formation of ceramic phase. The mechanical properties of the composites including bending strength and compressive strength both significantly ascended owing to the precipitation hardening heat treatment. An infiltration method for preparing boron carbide–aluminum ( $\text{B}_4\text{C}$ –Al) composite was modified so as to reduce the processing temperature and time [16]. Recently, ARSLAN et al [17] studied the phase composition of  $\text{B}_4\text{C}$ /Al composites infiltrated under different temperatures through the method of quantitative X-ray diffraction analysis. However, the effects of heat treatment on phase contents and mechanical properties of  $\text{B}_4\text{C}$ /2024Al composites have not been reported yet. In the present work, we have used pressureless infiltration approach to prepare  $\text{B}_4\text{C}$ -based composites infiltrated with molten 2024Al alloys and carefully investigated the phase contents and mechanical properties of the composites. The effects of heat treatment after infiltration on the phase contents and mechanical properties of the  $\text{B}_4\text{C}$ /2024Al composites were investigated, and the microstructure of the composites along with their mechanical mechanisms was also discussed.

## 2 Experimental

### 2.1 Materials and sample preparation

Commercially available  $\text{B}_4\text{C}$  powders with average particle size of  $3.5 \mu\text{m}$  (97% purity, supplied by Mudanjiang company) were used in the as-received state. Powders doped with polyvinyl alcohol were dry mixed for 16 h. Then the powders were uniaxially pressed (10 mm in height and 100 mm in diameter) into compacts in a steel die at 100 MPa. Green densities, calculated based on specimen dimensions and mass, were in the range of 60%–68% of theoretical density ( $2.52 \text{ g/cm}^3$ ). The compacts were pre-sintered under argon condition at  $1800 \text{ }^\circ\text{C}$  for 2 h.

Melt infiltration was done by placing 2024Al alloy pieces on the top of preforms. The chemical compositions of 2024Al alloy determined by ICP-OE are shown in Table 1. The preforms with metal pieces on their top were positioned in a graphite or corundum crucible, and then evacuated in furnace by pumping to 0.1 Pa vacuum prior to heating. The infiltration process was conducted at  $1200 \text{ }^\circ\text{C}$  for 60 min followed by furnace cooling. High-purity (99.99%) argon was used during infiltration. After being infiltrated, the composites were heat treated at the temperature of 660, 700, 800 or  $900 \text{ }^\circ\text{C}$  for 12, 24 or 36 h.

**Table 1** Nominal chemical composition of 2024 aluminum alloy (mass fraction, %)

Cu	Mg	Si	Fe	Mn
3.8–4.9	1.2–1.8	0.5	0.5	0.3–0.9
Cr	Zn	Ti	Others	Al
0.10	0.25	0.15	0.20	Bal.

### 2.2 Mechanical tests and characterization

Three-point-bending tests were carried out to measure flexural strength of the infiltrated  $\text{B}_4\text{C}$ –2519Al composites and the dimensions of the bars were  $35 \text{ mm} \times 4 \text{ mm} \times 3 \text{ mm}$  with a support span of 30 mm. The flexural strength is given by

$$\sigma_f = \frac{3FL}{2bh^2} \quad (1)$$

where  $F$  is the measured load at fracture;  $L$  is the support span distance;  $b$  is the width of the specimen; and  $h$  is the specimen thickness. All tests were performed using an Instron 3369 mechanical testing machine under a crosshead speed of  $0.5 \text{ mm/min}$ . The hardness of the  $\text{B}_4\text{C}$ –2024Al composites was evaluated by the Rockwell A indentations (HRA) using a standard A indentation tester. The Rockwell A diamond stylus (cone apex angle  $120^\circ$ , tip radius  $R=0.2 \text{ mm}$ ) was used to perform the tests. The applied load on the stylus was 60 kg. The density of the infiltrated composites was determined by the Archimedes method.

After the infiltrating and mechanical experiments, the selected specimens were sectioned and polished for microstructure observation using a electron probe X-ray microanalysis (EPMA, JXA8230), field emission scanning electron microscopy (FESEM) (FEI nano230 or quanta200) combined with an energy-dispersive spectrometer (EDS). The crystalline structure and contents of phases were characterized by X-ray diffraction (XRD) (Rigaku 3014) technique by  $\text{Cu K}\alpha$  radiation.

## 3 Results and discussion

### 3.1 Characterization of $\text{B}_4\text{C}$ preforms

Figure 1 shows the SEM images of porous  $\text{B}_4\text{C}$  preforms before and after pre-sintering.  $\text{B}_4\text{C}$  green preforms molded by pressing have sharp edges and corners before pre-sintering (Fig. 1(a)), and become interconnected to three-dimensional connected network skeleton structure after pre-sintering at  $1800 \text{ }^\circ\text{C}$  for 2 h. It is shown that the  $\text{B}_4\text{C}$  particles grow round and smooth from irregular shape after sintering (Fig. 1(b)). The results of XRD analysis of  $\text{B}_4\text{C}$  preforms after pre-sintering are shown in Fig. 2. It is found that  $\text{B}_4\text{C}$  is the main phase of ceramics skeleton, with a small amount of free carbon.

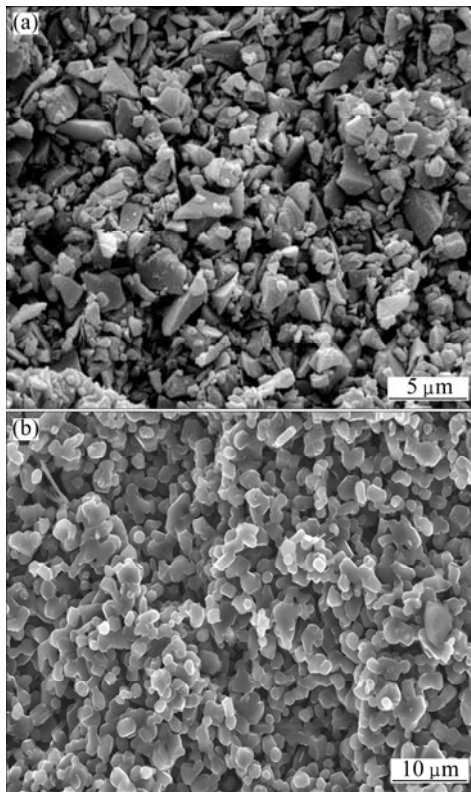


**Fig. 1** SEM images of B<sub>4</sub>C porous ceramics performs: (a) Before pre-sintering; (b) After pre-sintering

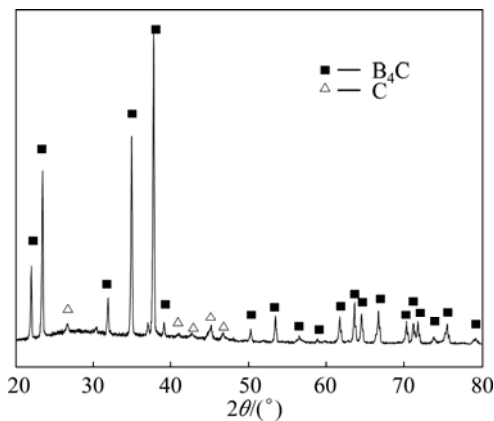


**Fig. 2** XRD pattern of B<sub>4</sub>C porous ceramics skeleton preform

### 3.2 Phase analysis of composites

Figure 3 shows the XRD patterns of B<sub>4</sub>C/2024Al composites prepared by pressureless infiltration methods. The primary phases of B<sub>4</sub>C/2024Al include B<sub>4</sub>C, Al, Al<sub>3</sub>BC and AlB<sub>2</sub>, with an extremely small amount of Al<sub>2</sub>Cu phase. It can be discovered that heat treatment at 800 °C for 36 h has exerted a significant impact on phase contents of the composites but has little influence on phase species. For further studies on the effects of heat treatment temperature on phase contents of the composites, quantitative analysis of XRD pattern of composites under a series of temperatures was also conducted.

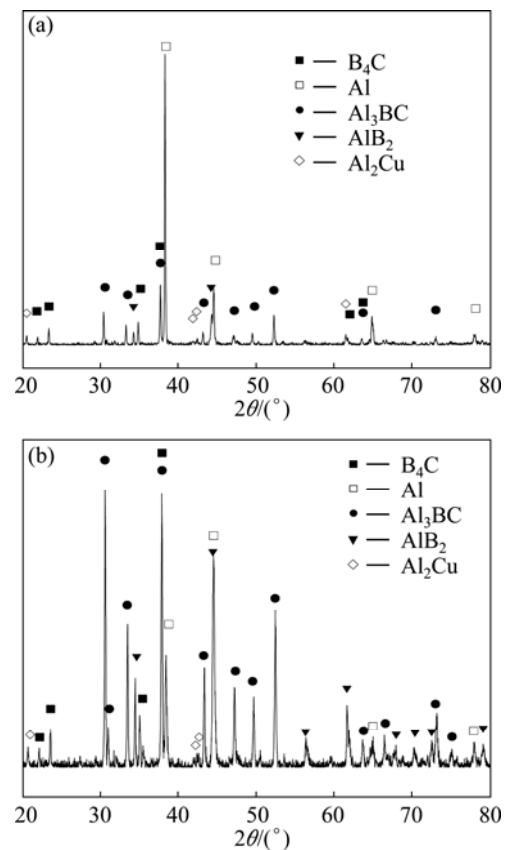


**Fig. 3** Typical XRD patterns of B<sub>4</sub>C/Al composites without heat treatment (a) and with heat treatment at 800 °C for 36 h (b)

The main purpose of XRD quantitative analysis was to measure the contents of every single phase of multiphase materials based on qualitative analysis, of which the theoretical basis is that diffraction intensity is proportional to the volume of substances participating in diffraction. The diffraction intensity ( $I$ ) of a single substance is [18]

$$I = \frac{1}{32\pi R} I_0 \frac{e^4}{m^2 c^4} \frac{\lambda^3}{V_0^2} V F_{HKL}^2 P \frac{1 + \cos^2(2\theta)}{\sin^2 \theta \cos \theta} e^{-2M} \frac{1}{2\mu} \quad (2)$$

where  $R$  is the distance between the sample diffraction rings;  $I_0$  is the intensity of incident X-ray;  $e$  and  $m$  are the electricity and mass of one electron, respectively;  $c$  is the speed of light;  $\lambda$  is the wavelength of incident X-ray;  $V_0$  is the volume of a unit cell;  $V$  is the volume of the irradiated powder sample;  $F_{HKL}$  is the structure factor;  $P$  is the multiple factor;  $2\theta$  is the diffraction angle;  $e^{-2M}$  is the temperature factor for adjustment of dispersion factor;  $\mu$  is linear absorption coefficient.

For multiphase substances [19],

$$I_j = CK_j \frac{w_j}{2\rho_j \sum_{j=1}^n w_j (\mu_m)_j} \quad (3)$$

where  $j$  is the phase  $j$  of all the  $n$  phases, and  $w_j$  is the

mass fraction of phase  $j$ ,  $C = \frac{1}{32\pi R} I_0 \frac{e^4}{m^2 c^4} \lambda^3$ ,

$$K_j = \frac{1}{V_0^2} F_{HKL}^2 P \frac{1 + \cos^2 2\theta}{\sin^2 \theta \cos \theta} e^{-2M}$$

Equation (3) is a generally applicable formula that describes the relationship between diffraction intensity of every single phase and its content in multiphase substances.

Supposed that contents of phase  $j$  are required to measure, taking one certain phase in the composites as internal standard substance “s”, the derivation is as follows:

$$\frac{I_j}{I_s} = K_s^j \frac{w_j}{w_s} \tag{4}$$

where  $K_s^j = \frac{K_j \rho_s}{K_s \rho_j}$ , which depends on the density and diffraction angle of the two phases, but not on their phase contents.  $K_j^i = K_s^i / K_s^j$ .

Based on the derivation above, the following equations can be deduced:

$$w_j = \frac{I_j w_s}{I_s K_s^j} \tag{5}$$

$$\sum_{j=1}^n w_j = 1 \tag{6}$$

Accordingly, phase contents of multiphase substances can be calculated.

In Ref. [16], Si acted as the reference substance, and mixed samples of pure Al, B<sub>4</sub>C, AlB<sub>2</sub> and Si were prepared to calculate the Si reference intensity to the three substances above. Then reference intensity  $K_{Si}^X$  could be calculated from the slope of intensity ratio against mass ratio, where  $X$  stands for phase formula. According to the results of Ref. [17], the reference intensity ratios (RIR) of pure Al, B<sub>4</sub>C, AlB<sub>2</sub> to Si are as follows:

$$K_{Si(111)}^{Al(111)} = 1.02, \quad K_{Si(111)}^{B_4C(104)} = 0.071, \quad K_{Si(111)}^{AlB_2(100)} = 0.118.$$

$$\text{Accordingly, } K_{Al(111)}^{B_4C(104)} = K_{Si(111)}^{B_4C(104)} / K_{Si(111)}^{Al(111)} = 0.0696,$$

$$K_{Al(111)}^{AlB_2(100)} = K_{Si(111)}^{AlB_2(100)} / K_{Si(111)}^{Al(111)} = 0.1157.$$

From PDF card, the RIR values of Al<sub>3</sub>BC and Si to  $\alpha$ -Al<sub>2</sub>O<sub>3</sub> are  $K_{\alpha-Al_2O_3(113)}^{Al_3BC(101)} = 1.17$ ,  $K_{\alpha-Al_2O_3(113)}^{Si(111)} = 4.55$ , so

$$K_{Al(111)}^{Al_3BC(101)} = K_{\alpha-Al_2O_3(113)}^{Al_3BC(101)} / K_{\alpha-Al_2O_3(113)}^{Si(111)} / K_{Si(111)}^{Al(111)} = 0.252.$$

XRD intensity generally refers to the integrated intensity represented by the area of main peak, while quantitative phase analysis is based on integrated intensity ratio. However, since the XRD peak height ratio approximately equals integrated intensity ratio [19], it's often a substitution when integrated intensity ratio of

each phase is required. Intensity of XRD peak of specific crystal surface of each phase, which is shown in Table 2, can be calculated by selecting value from XRD spectra of composites heat-treated at different conditions. When relative content is extremely small, the phase content of Al<sub>2</sub>Cu is ignored in quantitative phase analysis.

**Table 2** Effect of heat treatment on intensity of diffraction peaks of each phase in B<sub>4</sub>C/2024Al composites (heat preservation time 36 h)

Temperature/°C	$I_{Al(111)}$	$I_{Al_3BC(101)}$	$I_{AlB_2(100)}$	$I_{B_4C(104)}$
No heat treatment	3749	431	174	304
660	693	735	298	279
700	683	1106	419	374
800	382	945	304	178
900	868	1055	399	363

Based on the derivation above, through calculating, the contents of each phase of B<sub>4</sub>C/2024Al composites before and after heat-treatment are obtained, as shown in Table 3. To more intuitively demonstrate the effects of different heat-treatment temperatures on phase content of B<sub>4</sub>C/2024Al composites, Table 3 is transferred to Fig. 4.

**Table 3** Effect of heat treatment on phase content of B<sub>4</sub>C/2024Al composites

Temperature/°C	w(Al)/%	w(Al <sub>3</sub> BC)/%	w(AlB <sub>2</sub> )/%	w(B <sub>4</sub> C)/%
No heat treatment	33.1	15.1	13.2	38.6
660	8.1	28.6	25.2	38.1
700	4.9	31.2	25.7	38.2
800	4.1	40.2	28.1	27.4
900	6.3	30.5	25.1	38.1

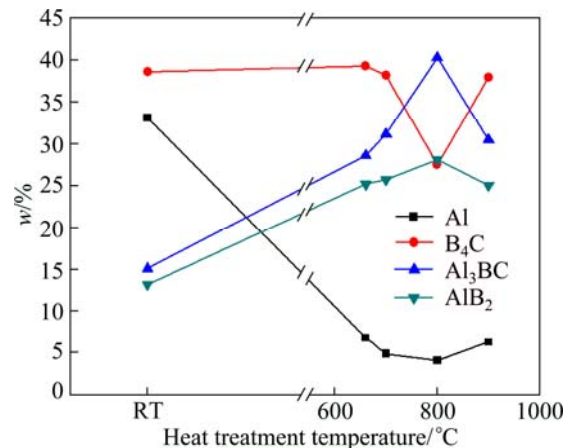


**Fig. 4** Quantitative X-ray diffraction analysis results of B<sub>4</sub>C/2024Al composites

Figure 4 and Table 3 show that phase content of the composites changed considerably due to heat treatment.

During pressureless infiltration processed at high temperatures,  $B_4C$  reacted with Al to form a certain amount of  $Al_3BC$  and  $AlB_2$ , of which the chemical equation is



The reaction rate decreased with the forming of ceramic intermediate phase and encapsulated  $B_4C$  particles, and the reaction ended when the coating intermediate phases became dense enough [12,13].

However, heat treatment can create conditions for the reaction to continue. After heat treatment, phase contents of  $B_4C$  and Al gradually decreased while those of  $Al_3BC$  and  $AlB_2$  increased (Fig. 4). Contents of both reactants and products spontaneously reached their extreme value after heat treatment at 800 °C for 36 h. Phase contents after heat treatment at 900 °C for 36 h were close to those at 700 °C. Below 800 °C, intermediate phase surrounding  $B_4C$  particles is not dense enough. The diffusion rate increased as temperature increased, resulting in more and more ceramic intermediate phase forming. When the intermediate phase became dense enough, the reaction ended. At the temperature of 900 °C, the dense encapsulation layer prevented the reaction process extremely; therefore, the content of ceramic intermediate phase at 900 °C is lower than that at 800 °C.

To more clearly observe the effects of heat treatment, the microstructure and phase contents of  $B_4C/2024Al$  composites were analyzed by means of electron probe X-ray microanalysis (EPMA). EPMA images of  $B_4C/2024Al$  composites before and after heat treatment are presented in Fig. 5. There are five contents in Fig. 5(a), which could be determined, combined with content analysis, to be Al,  $Al_3BC$ ,  $AlB_2$ ,  $B_4C$ , and  $Al_2Cu$ . For the reaction was not thorough, the content of ceramic intermediate phase is low, while  $B_4C$  and Al occupying a relatively large area. Figure 5(b) demonstrates that after heat treatment at 800 °C for 36 h, the chemical reaction was nearly completed, ceramic intermediate phase encapsulated the black  $B_4C$  particles to prevent them from contacting Al.  $B_4C$  particles remain separately, and phase contents of  $B_4C$  and Al are significantly lower than those of as-products, which was consistent with the results of X-ray quantitative analysis.

### 3.3 Mechanical properties of composites

$B_4C/Al$  composites are potentially applied to bulletproof panel, of which hardness is the principal mechanical parameter. Hardness test results of the  $B_4C/2024Al$  composites under different heat-treatment conditions are presented in Fig. 6. Remaining temperature unchanged, hardness of composites has a tendency of increase with lengthening time. At the same

time, it increases with the rising temperature. Hardness of the composites reaches its maximum value at heat-treatment temperature of 800 °C, and lowers slightly at 900 °C.

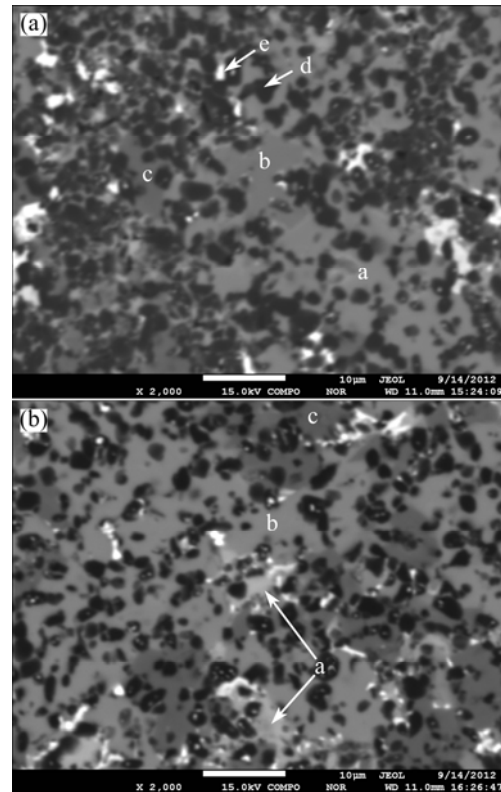


Fig. 5 EPMA images of  $B_4C/Al$  composites: (a) No heat treatment; (b) Heat treatment at 800 °C for 36 h (a–Al; b– $Al_3BC$ ; c– $AlB_2$ ; d– $B_4C$ ; e– $Al_2Cu$ )

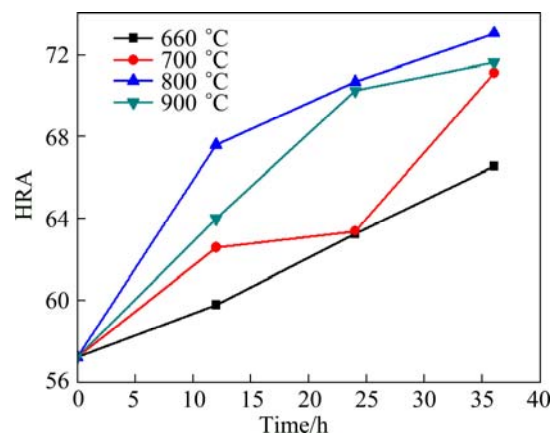
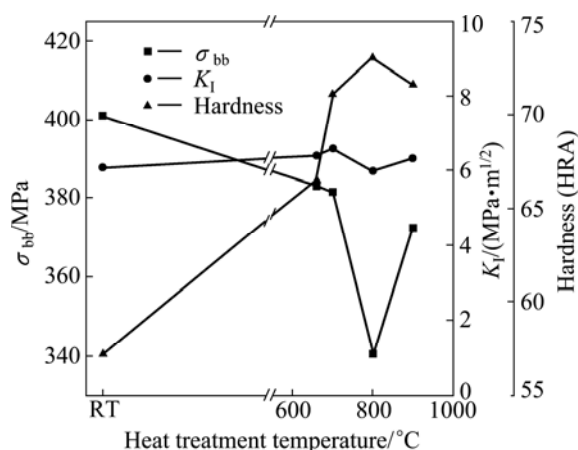


Fig. 6 Hardness of  $B_4C/Al$  composites after heat treatment

The content of each phase has an impact on hardness of the substance. As is reported in previous references, the magnitude relation of hardness in  $B_4C/Al$  composites is as follows:  $B_4C > Al_3BC > AlB_2 > Al$  [20]. The results of quantitative phase analysis reveal that at 800 °C, a large number of ceramic intermediate phases exist in the composites, among which the content of Al is

the lowest, causing the composites to obtain the highest hardness. Composites heat-treated at 800 °C have the maximum amount of reaction products  $\text{Al}_3\text{BC}$  and  $\text{AlB}_2$ , at the same time, the minimum amount of reactants  $\text{B}_4\text{C}$  and Al. And this is proved in Fig. 5(b), from which it can be seen that chemical reactions are nearly completed.

To more comprehensively assess the mechanical properties of  $\text{B}_4\text{C}/2024\text{Al}$  composites, the bending strength and fracture toughness after heat treatment were tested, as shown in Fig. 7. Bending strength decreases through heat treatment, but fracture toughness is slightly influenced. The considerable consumption of plastic metal, Al alloy, contributes to the decrease of bending strength and fracture toughness. With a large amount of Al alloy added, the composites obtain relatively higher bending strength (401 MPa) and fracture toughness ( $6.1 \text{ MPa}\cdot\text{m}^{1/2}$ ), but lower hardness (HRA57.3). After heat treatment at 800 °C for 36 h, the composites have the largest amount of  $\text{Al}_3\text{BC}$  and  $\text{AlB}_2$ , which contributes to the highest hardness (HRA73.1), as well as the least amount of  $\text{B}_4\text{C}$  and Al, thus obtaining considerably decreased bending strength along with a certain decrease in fracture toughness. After heat treatment at 700 °C for 36 h, the composites obtain the best overall mechanical properties, hardness reaching HRA71.1, bending strength ( $\sigma_{\text{bb}}$ ) 382 MPa and fracture toughness ( $K_{\text{I}}$ )  $6.58 \text{ MPa}\cdot\text{m}^{1/2}$ .



**Fig. 7** Effect of heat treatment for 36 h on mechanical properties of  $\text{B}_4\text{C}/\text{Al}$  composites

The bending strength of composites depends on the  $\text{B}_4\text{C}$  matrix as volume fraction of Al in the composites is extremely low. Fracture of  $\text{B}_4\text{C}$  ceramics is based on the defects that exist inside or on the surface of the composites. The existence of defects is probabilistic, and as the probability increases, bending strength composites decreases. Besides, the probability of fracture can be calculated according to the Weibull function, based on the theory of the weakest link. Once the micro cracks propagate to their threshold sizes,  $\text{B}_4\text{C}$  matrix cracks

rapidly and then shears Al, thereby the composites become invalid.

Bending strength of composites is related to crystal boundary. Once the cohesion between reaction products is not adequately close, they become micro crack source when loads are exerted to the composites. As the cracks gradually propagate, the  $\text{B}_4\text{C}$  matrix cracks easily at the same time. And based on the fact that bending strength of the composites depends on  $\text{B}_4\text{C}$  matrix, it decreases substantially as a result.

Above all, the excessive insoluble particles and precipitated phases become micro crack source as they perform poor cohesion with the  $\text{B}_4\text{C}$  matrix. When exerted loads, the matrix cracks easily and eventually the bending strength of composites decreases considerably with the crack propagation.

As shown in Fig. 7, composites exerted heat treatment of 800 °C perform significantly lower bending strength compared with 700 °C and 900 °C. As is previously analyzed, the reactions of the composites are nearly completed under heat treatment of 800 °C, which causes large consumption of  $\text{B}_4\text{C}$  matrix, bending strength of the composites drops thereby.

The results also demonstrate that fracture toughness of the composites changed slightly regardless of the temperature of heat treatment. After heat treatment, the amount of crystal boundary between the reaction products and  $\text{B}_4\text{C}$  matrix does not decrease, therefore, the energy consuming function still works, allowing the fracture toughness of composites to remain steady.

## 4 Conclusions

1)  $\text{B}_4\text{C}/2024\text{Al}$  composites were successfully produced by pressureless infiltration method. The porous ceramics skeleton preforms were prepared by pre-sintering at 1800 °C for 2 h under argon condition, and the  $\text{B}_4\text{C}$  porous ceramics preforms were infiltrated by molten 2024 aluminum alloy at 1200 °C to prepare  $\text{B}_4\text{C}/2024\text{Al}$  composites.

2) The phases of  $\text{B}_4\text{C}/2024\text{Al}$  composites include  $\text{B}_4\text{C}$ , Al,  $\text{Al}_3\text{BC}$ ,  $\text{AlB}_2$  and  $\text{Al}_2\text{Cu}$ . The phase species remain unchanged, while phase contents of the composites change significantly owing to the heat treatment. The contents of intermediate phases of  $\text{Al}_3\text{BC}$ ,  $\text{AlB}_2$  increased largely after heat treatment and reached the maximum value after heat treatment at 800 °C for 36 h.

3) Heat treatment results in not only considerable enhancement in hardness, but also reduction in bending strength of the composites. Bending strength decreases through heat treatment, but fracture toughness is slightly influenced. Composites heat treated at 800 °C for 36 h have the highest hardness of HRA73.1, while those

under 700 °C for 36 h have the best comprehensive mechanical properties.

## References

- [1] MASHHADI M, EHSAN T N, VINCENZO M S. Pressureless sintering of boron carbide [J]. *Ceramics International*, 2010, 36: 151–159.
- [2] MIYAZAKI H, ZHOU Y, HYUGA H. Microstructure of boron carbide pressureless sintered in an Ar atmosphere containing gaseous metal species [J]. *Journal of European Ceramic Society*, 2010, 30: 999–1005.
- [3] THEVENOT F. A review on boron carbide [J]. *Journal of European Ceramic Society*, 1990, 6: 205–225.
- [4] LI Chong-jun, MA Bo-xin, WANG Kang-li. Preparation of aluminum matrix composite by pressureless infiltration process [J]. *Rare Metals*, 1998, 17: 5–9.
- [5] LI Chong-jun, JIN Zhi-hao, MA Bo-xin, HAO Zhi-biao. Properties of aluminum matrix composite by pressureless infiltration [J]. *Journal of Xi'an Jiaotong University*, 1999, 33: 68–71. (in Chinese)
- [6] YAMANAKA T, CHOI Y B, MATSUGI K, YANAGISAWA O, SASAKI G. Influence of preform preparation condition on infiltration of molten aluminum [J]. *Journal of Materials Processing Technology*, 2007, 187–188: 530–532.
- [7] CANAKCI A, VAROL T. Production and microstructure of AA2024-B<sub>4</sub>C metal matrix composites by mechanical alloying method [J]. *Usak University Journal of Material Sciences*, 2012, 1(1): 15–22.
- [8] HALVERSON D C, PYZIK A J, AKSAY A, SNOWDEN W E. Processing of boron carbide–aluminium composites [J]. *Journal of the American Ceramic Society*, 1989, 72(5): 775–780.
- [9] KISASOZ A, GULER K A, KARAASLAN A. Infiltration of A6063 aluminium alloy into SiC–B<sub>4</sub>C hybrid preforms using vacuum assisted block mould investment casting technique [J]. *Transactions of Nonferrous Metals Society of China*, 2012, 22(7): 1563–1567.
- [10] WESTERMANN I, HAUGSTAD A L, LANGSRUD Y, MARTHINSEN K. Effect of quenching rate on microstructure and mechanical properties of commercial AA7108 aluminium alloy [J]. *Transactions of Nonferrous Metals Society of China*, 2012, 22(8): 1872–1877.
- [11] PYZIK A J, OTT J J, CARROLL D F, PRUNIER A R. Method of preparing boron carbide/aluminum cermets having a controlled microstructure: US 5394929 [P]. 1995–03–07.
- [12] VIALA J C, BOUIX J, GONZALEZ G. Chemical reactivity of aluminum with boron carbide [J]. *Journal of Material Science*, 1997, 32: 4559–4573.
- [13] LÜ P, YUE X Y, YU L. Effect of in situ synthesized TiB<sub>2</sub> on the reaction between B<sub>4</sub>C and Al in a vacuum infiltrated B<sub>4</sub>C–TiB<sub>2</sub>–Al composite [J]. *Journal of Material Science*, 2009, 44: 3483–3487.
- [14] LEE B S, KANG S. Low-temperature processing of B<sub>4</sub>C–Al composites via infiltration technique [J]. *Materials Chemistry and Physics*, 2001, 67: 249–255.
- [15] TUNCER N, TASDELEN B, ARSLAN G. Effect of passivation and precipitation hardening on processing and mechanical properties of B<sub>4</sub>C–Al composites [J]. *Ceramics International*, 2011, 37: 2861–2867.
- [16] JUNG J, KANG S. Advances in manufacturing boron carbide–aluminum composites [J]. *Journal of American Ceramic Society*, 2004, 87: 47–54.
- [17] ARSLAN G, KARA F, TURAN S. Quantitative X-ray diffraction analysis of reactive infiltrated boron carbide–aluminium composites [J]. *Journal of European Ceramic Society*, 2003, 23: 1243–1255.
- [18] FRAGE N, LEVIN L, FRUMIN N. Manufacturing B<sub>4</sub>C–(Al,Si) composite materials by metal alloy infiltration [J]. *Journal of Materials Processing Technology*, 2003, 143–144: 486–490.
- [19] LI Shu-tang. *Crystal X-ray diffraction basis* [M]. Beijing: Metallurgical Industry Press, 1990. (in Chinese)
- [20] HALVERSON D C, PYZIK A J, AKSAY I A. Boron–carbide–aluminum and boron–carbide–reactive metal cermets: US 4605440 [P]. 1986–08–12.

# 热处理对无压浸渗法制备 B<sub>4</sub>C/2024Al 复合材料相组成及力学性能的影响

谭孝芬<sup>1</sup>, 曾凡浩<sup>1</sup>, 王抒秋<sup>1</sup>, 周飞<sup>2</sup>, 熊翔<sup>1</sup>

1. 中南大学 粉末冶金研究院 粉末冶金国家重点实验室, 长沙 410083;

2. 中南大学 材料科学与工程学院, 长沙 410083

**摘要:** 利用无压浸渗法制备 B<sub>4</sub>C/2024Al 复合材料, 并通过 XRD、SEM 和力学性能检测研究热处理对复合材料相组成以及材料性能的影响。结果表明, B<sub>4</sub>C/2024Al 复合材料包含 B<sub>4</sub>C、Al、Al<sub>3</sub>BC、AlB<sub>2</sub> 和 Al<sub>2</sub>Cu 相。经过 660、700、800 和 900 °C 热处理 12、24 或 36 h 后, 相种类并没有变化, 但是相含量发生显著改变。此外, 经热处理, 材料的硬度得到显著提高, 抗弯强度有所下降。经 800 °C 热处理 36 h 的材料硬度最高, 经 700 °C 热处理 36 h 的材料具有最优良的综合性能。

**关键词:** B<sub>4</sub>C/2024Al 复合材料; 热处理; 无压浸渗法; 硬度; 抗弯强度

(Edited by Xiang-qun LI)